Renewable Energy 36 (2011) 2278–2286

Contents lists available at ScienceDirect

Renewable Energy

journal homepage: www.elsevier.com/locate/renene

A Monte Carlo approach to generator portfolio planning and carbon emissions assessments of systems with large penetrations of variable renewables

Elaine K. Hart*, Mark Z. Jacobson

Department of Civil and Environmental Engineering, Stanford University, 473 Via Ortega, MC 4020, Stanford, CA 94305, USA

ARTICLE INFO

Article history:
Received 28 September 2010
Accepted 13 January 2011

Keywords:
Renewable energy
Intermittent generation
Wind power
Solar power
Carbon emissions

ABSTRACT

A new generator portfolio planning model is described that is capable of quantifying the carbon emissions associated with systems that include very high penetrations of variable renewables. The model combines a deterministic renewable portfolio planning module with a Monte Carlo simulation of system operation that determines the expected least-cost dispatch from each technology, the necessary reserve capacity, and the expected carbon emissions at each hour. Each system is designed to meet a maximum loss of load expectation requirement of 1 day in 10 years. The present study includes wind, centralized solar thermal, and rooftop photovoltaics, as well as hydroelectric, geothermal, and natural gas plants. The portfolios produced by the model take advantage of the aggregation of variable generators at multiple geographically disperse sites and the incorporation of meteorological and load forecasts. Results are presented from a model run of the continuous two-year period, 2005–2006 in the California ISO operating area. A low-carbon portfolio is produced for this system that is capable of achieving an 80% reduction in electric power sector carbon emissions from 2005 levels and supplying over 99% of the annual delivered load with non-carbon sources. A portfolio is also built for a projected 2050 system, which is capable of providing 96% of the delivered electricity from non-carbon sources, despite a projected doubling of the 2005 system peak load. The results suggest that further reductions in carbon emissions may be achieved with emerging technologies that can reliably provide large capacities without necessarily providing positive net annual energy generation. These technologies may include demand response, vehicle-to-grid systems, and large-scale energy storage.

1. Introduction

In the United States, approximately 40% of the total annual carbon dioxide emissions are associated with the generation of electricity [1]. Significant reductions in carbon emissions within the United States will therefore require a dramatic shift in the composition of the electric power sector. Several technologies already exist to replace generation from coal and natural gas with cleaner alternatives, but the variability and uncertainty in many renewable resources is anticipated to pose political, financial, and technological challenges to large-scale grid integration. Without practical examples of large systems with very high penetrations of variable generation, models must be employed to predict the behavior of these systems. To date, most grid integration models have focused on wind power, though some have included solar technologies. An extensive review of wind power integration studies across Europe can be found in [2] and a review of current energy system modeling tools can be found in [3].

Early attempts at modeling grid integration of variable generation were based on load duration curve analyses, similar to those used for portfolios of conventional generators [4–6]. More recently, however, grid integration has been formulated primarily as an optimization problem with load balance constraints over multiple time steps. Deterministic load balance models have been used to develop scenarios with high penetrations of wind power within different types of preexisting generation portfolios [7], to study the affects of aggregating multiple geographically disperse wind farms [8], and to analyze the operational costs associated with intrahour fluctuations of wind power output [9]. Other grid integration studies have explored how the complementary nature of different renewable energy resources (including wind, solar, wave, geothermal, and/or hydroelectric power) can be used to best match a time-varying power demand [10–16].

The stochastic nature of wind and solar complicates the treatment of system reliability in grid integration studies. Probabilistic models are already used to account for forced outages of

* Corresponding author. Tel.: +1 650 721 2650; fax: +1 650 7237058.
E-mail address: ehart@stanford.edu (E.K. Hart).

0960-1481/$ – see front matter © 2011 Elsevier Ltd. All rights reserved.
doi:10.1016/j.renene.2011.01.015

conventional plants in analyzing system reliability, but these have yet to be widely applied to variable generators with uncertain resource availability. Models that assume that generation from wind and solar facilities is completely deterministic may neglect the additional strain that forecast uncertainty adds to the system, while those that do not include meteorological forecasts potentially overestimate the costs associated with grid integration. These issues are subtleties for low penetrations of variable renewables, but may become major design factors for highly intermittent generation portfolios. The WILMAR model includes a particularly robust treatment of the uncertainty in wind power availability by formulating the grid operation problem as a stochastic linear program [17,18]. In the WILMAR model, wind power forecast errors are accounted for by producing a number of potential wind power forecasts via a Monte Carlo method, similar to the methods used in this study for producing wind speed, irradiance, load, and forced outage realizations. Other studies with treatments of the stochastic nature of wind power in grid integration include Refs. [19–21]. Few studies have included an analysis of the carbon emissions associated with grid integration. Katzenstein and Apt provide one exception, with their study on the emissions associated with firming up wind and solar power with natural gas to provide baseload power [22].

The goal of the present study is to build on this body of work to develop a new generator portfolio planning tool. The model presented in this study utilizes the aggregation of geographically and technologically diverse variable renewables and meteorological and load forecasts to design systems capable of meeting time-dependent loads with a specified reliability. These systems are characterized by the composition of their generator portfolios and the expected carbon emissions associated with system operation. The model provides analyses of systems with very high penetrations of renewables and quantifies the ability of variable renewables to both displace carbon-based dispatchable generation and to reduce the carbon emissions associated with electric power generation.

2. Methodology

The model discussed here combines a deterministic planning optimization module with a Monte Carlo simulation of system operation (See Fig. 1). These modules are described in detail in Sections 2.4 and 2.5. Given historical or modeled system-wide hourly load data and site-specific hourly wind speed, irradiance, and temperature data, the model produces a renewable portfolio and calculates the following output: the installed capacities and capacity factors of renewable and conventional generators; the expected annual system-wide emissions; the expected levelized cost of generation; and additional information about system operation, including wind and solar curtailment statistics. Both modules rely on simplified linear models of each of the generator technologies, which are described in the following sections. Generation technologies are classified as baseload, dispatchable, or variable, depending on their availability and flexibility.

2.1. Baseload generators

Baseload generators in the model operate at a constant power output that is equal to the installed capacity, except in the case of forced outages in the stochastic simulation. In the present study, only geothermal power is assumed to operate as baseload. Geothermal generation in the deterministic optimization is therefore equal to the total geothermal installed capacity, which is an optimization variable subject to a constraint on the total resource availability.

2.2. Dispatchable generators

The term dispatchable is applied to conventional technologies that can be used to balance the load. In this study, these technologies include natural gas and hydroelectric plants. The fleet of natural gas generators is represented by two types of plants that differ in their day-ahead scheduling schemes. Class I plants are scheduled on a day-ahead basis in order to load balance given day-ahead meteorological and load forecasts. These plants are intended to deal with the forecastable variability of the load and generation. Class II plants, which are included to account for the stochastic nature of the load and generator availability, operate as spinning reserves, capable of responding to real-time meteorological and load forecasting errors. The available capacity of Class II plants in each hour is the minimum of the Class II installed capacity and the total forecasted load in that hour. The roles of Class I and II natural gas plants are illustrated by a comparison of the scheduled generation with real-time dispatch in Fig. 2. Both classes of plants are capable of ramping down to 0 and up to the maximum scheduled capacity in each time step. The emissions associated with the operation of the natural gas fleet are calculated using an empirically-derived emissions equation for the Westinghouse 501FD turbine from [22]:

$$E(t) = 0.2528P(t) + 17.46N(t) \quad (1)$$

where $E(t)$ is the emissions rate in tCO_2/hr, $P(t)$ is the power output in MW, and $N(t)$ is the number of turbines operating at time t, which is described by Eq. (2).

$$N(t) = ceil\left(\frac{P(t)}{P_{turb}}\right) \quad (2)$$

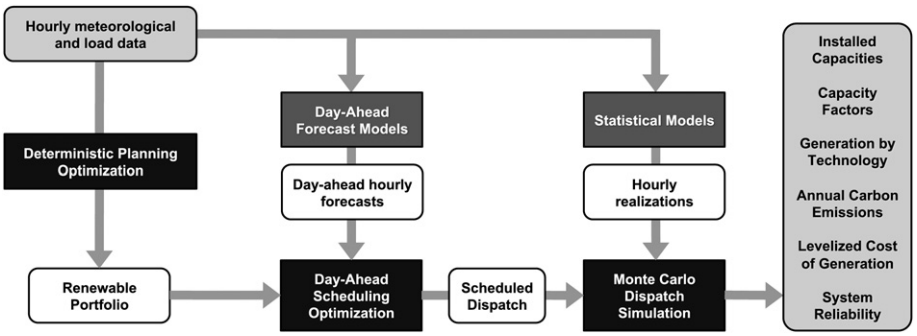

Fig. 1. Schematic of modeling approach.

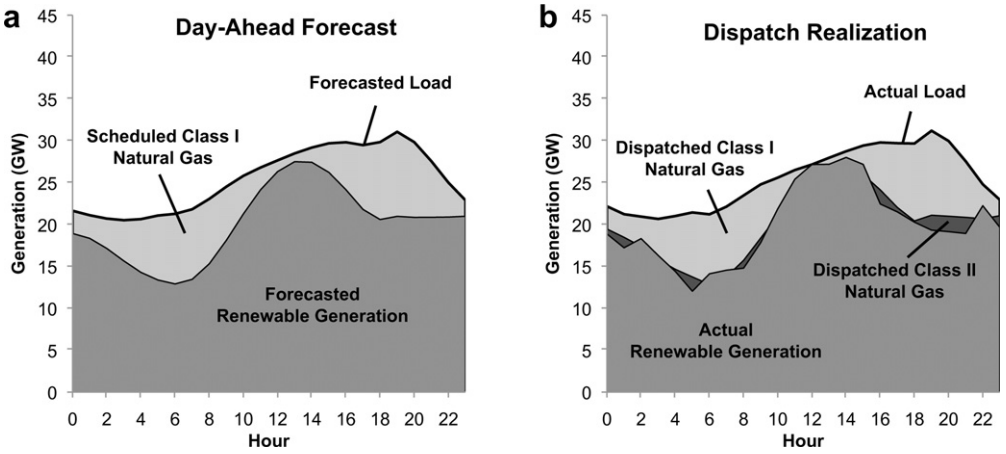

Fig. 2. Comparison of possible scheduled generation with Class I natural gas plants and one possible corresponding real-time dispatch. Class II natural gas plants are dispatched in real-time to mitigate day-ahead forecast errors.

where P_{turb} is the average turbine size in MW. Both types of natural gas plants assume a ramp rate limit consistent with the specifications of the Westinghouse 501FD turbine. Note that the natural gas plants considered by the deterministic planning optimization are assumed to operate as spinning reserves in order to ensure convexity, but the installed capacities, annual generation, and emissions of both classes of plants are recalculated in the Monte Carlo simulation.

Hydroelectric plants are broken into three classes: large-scale plants with storage, small hydroelectric plants, and pumped-storage facilities. Output from large-scale hydroelectric plants is scheduled on a day-ahead basis and is constrained by the total installed capacity of large hydroelectric plants and the estimated historical daily generation on that day. This ensures that the solution accounts for the seasonal fluctuations in the availability of hydroelectric power due to both meteorological effects and human use. Small hydroelectric plants are assumed to operate as baseload generators on each day, where the daily power output changes seasonally based on historical data. Output from pumped-storage facilities in the model is limited by the total installed capacity of pumped-storage and by an additional constraint that requires that the total daily generation is equal to zero for all days in the simulation period. The model assumes no additional development of hydroelectric facilities beyond 2006.

2.3. Variable generators

Variable generator technologies include wind power, solar thermal generation with thermal energy storage, and distributed photovoltaics. The wind generation model uses a REPower MM92 turbine power curve to compute maximum power output per turbine at each hour from 100-m wind speed data [23]. The model also assumes that wind power can be curtailed on an hourly basis in order to balance the system load. Future studies will include energy storage as an alternative to curtailment. In both the deterministic planning model and the dispatch model these assumptions reduce to the simple linear constraint:

$$P_i^W(t) \le W_i \times g(v_i(t)) \tag{3}$$

where $P_i^W(t)$ is the power output at the ith wind farm at time t, W_i is the installed capacity of the ith wind farm, $g(v)$ is a function that maps the wind speed to the fraction of maximum power output for a single turbine based on the turbine's power curve, and $v_i(t)$ is the 100-m wind speed.

The solar thermal model assumes that all solar thermal plants utilize single-axis tracking parabolic trough technology, with thermal energy storage (TES) systems that can dump excess energy if necessary. The model reduces to the following linear constraint:

$$S(t) - \eta_S S(t-1) \le \sum_j \left[\eta_{\text{collect}} A_j I_j^{ST}(t) - \frac{P_j^{ST}(t)}{\eta_{\text{turb}}} \right] \tag{4}$$

where η_S is the fraction of the stored energy that remains after one time step, η_{collect} is the fraction of the collectable solar power that is transferred to steam, η_{turb} is the turbine efficiency, A_j is the area of the jth solar field, $P_j^{ST}(t)$ is the power output, and $S(t)$ is the total energy stored in all the TES systems, which is approximated from experimental data on a single thermocline tank designed for use with parabolic trough solar thermal systems [24]. Both the turbine size and the array size are optimization variables, so that turbines can be undersized or oversized for the solar array. The irradiance that is collected by the parabolic trough array, $I_j^{ST}(t)$, is a function of the direct normal irradiance (DNI), the location, and the time of year (see Supplemental Information and [25] for more details). The present study assumes that the TES storage capacity is large enough to provide 3 h of rated power output. A 2-h time delay between sunrise and the availability of thermal energy from the collector field is also introduced to allow the system to warm up each morning.

The model includes residential rooftop photovoltaics that are south-facing at a tilt angle equal to the latitude and commercial photovoltaics that have zero tilt angles. Photovoltaic power output depends only on the installed capacity, the irradiance, and the temperature at each site:

$$P^{PV}(t) = \sum_j \frac{V_j I_j^{PV}(t) \eta_j^T(t) \eta_{PV}}{1000\ \text{W/m}^2} \tag{5}$$

where V_j is the installed capacity (in terms of dc rated power at standard test conditions) at the jth photovoltaic site, $I_j^{PV}(t)$ is the irradiance in W/m^2 that strikes the panels at time t at this site, $\eta_j^T(t)$ is an efficiency parameter that is related to temperature losses, and η_{PV} is an efficiency parameter that accounts for losses associated with mismatch, dirt, and the inverter. The irradiance, $I_j^{PV}(t)$, is a function of the direct normal irradiance, the diffuse horizontal irradiance (DHI), the site location, the time of year, and the tilt angle (see Supplemental Information and [25] for more details).

Because irradiance data are not available for every potential photovoltaic development site and because inclusion of all

potential sites would substantially increase the problem size, the model aggregates available solar data by county and assumes that the same fraction of the development potential is realized in each county. This reduces the photovoltaic model to two variables in the planning optimization problem: the total system-wide installed capacities of residential and commercial rooftop photovoltaics. Power output from photovoltaic systems is not subjected to transmission and distribution losses in the model, as it is assumed that most of the generation is used at or near the generation site.

2.4. Deterministic renewable portfolio planning model

The deterministic renewable portfolio planning problem is posed as a linear program. For low-cost portfolios, the total annual cost of generation (including annualized capital cost, fixed and variable O&M costs, and fuel costs) is minimized. Alternatively, low-carbon portfolios can be produced by minimizing the estimated annual carbon emissions, a linear function of the installed capacity of and the annual generation from natural gas plants. The minimization is subject to a power balance constraint that ensures that the generation (minus a constant fractional transmission and distribution loss term) equals the load at every hour. The optimization variables include: total installed capacities of each generation technology, site-specific installed capacities of wind and solar thermal plants, hourly generation from each technology, and hourly total energy stored in the TES systems at the solar thermal plants. Additional linear constraints are included in the renewable portfolio optimization based on the generator models described in the preceding sections and land/resource availability data. The linear program is solved using CVX, a modeling system built on top of MATLAB that solves convex optimization problems [26,27].

Because the hourly generation from each technology is a variable in the optimization, the size of the optimization scales with the length of the time period under consideration. Rather than considering all time steps in the simulation time horizon, the problem size is reduced significantly by selecting 20 random days to characterize typical system behavior and eight specific days that contain hours with extreme meteorological and load events. To calculate annual cost and emissions, weights for each day are assigned using least-squares to best match the annual load, wind speed, and irradiance distributions.

2.5. Monte Carlo dispatch simulation

The dispatch module uses the installed capacities from the deterministic planning optimization and a set of load and meteorological realizations built from historical data, modeled data, and simple statistical models to simulate potential dispatch scenarios. The module includes a day-ahead scheduling optimization and an hourly dispatch optimization. The day-ahead 24-h schedule of Class I natural gas, large-scale hydro, and pumped-storage hydro is produced by solving a least-cost dispatch optimization problem at 1 pm of each day in the simulation using meteorological and load forecasts for the following day. An additional constraint requires that no more than 65% of the scheduled generation in each hour come from these inflexible generators in order to prevent overgeneration. At each hour, the hourly dispatch optimization then determines the dispatch schedule for the next 24 h that minimizes the expected cost of generation based on meteorological and load forecasts, scheduled generation, and current conditions (which give rise to forecast errors and forced outages). The first hour of the dispatch solution gives the real-time dispatch for the hour of interest. An additional term in the dispatch optimization allows for a relatively expensive deficit in hours when the available generation does not meet the demand. This hourly deficit is used after the dispatch simulation completes to calculate the capacity of and generation from Class II natural gas plants that is required for the system to meet the load with a loss of load expectation of 1 day in 10 years.

The Monte Carlo simulation relies on the assumption that meteorological processes, demand fluctuations, and forced outages can be approximated as Markov chain processes. Given this assumption, simple statistical models are used to produce meteorological and load realizations for the Monte Carlo simulation. Wind speed realizations are produced using an algorithm that includes treatments of the temporal and geographic correlations and any diurnal character present in the wind speed dataset. Because statistical studies of day-ahead wind speed forecasts have primarily reported the error of the mean daily wind speed forecast, the wind speeds for the k^{th} realization are produced first by randomly generating the mean daily wind speed, $u_{i,k}(d)$ on each day, d, and each wind development site, i:

$$u_{i,k}(d) = \widehat{u}_i(d) + \tilde{x}_i \tag{6}$$

where $u_{\ i}(d)$ is the forecasted mean daily wind speed, $\tilde{x}_i \sim \mathcal{N}(0, \sigma_W^2)$, and σ_W is the presumed rms error of the day-ahead mean daily wind speed forecasts (25%). Realizations of the random variable $\tilde{x}_i$ are generated using the Cholesky decomposition of the correlation matrix built from site-specific mean daily wind speed data. This approach maintains any geographical correlations due to proximity or weather phenomena that are present in the wind dataset. Diurnal character is imposed by a function, $\alpha_i(t)$, which gives the monthly-averaged ratio of the wind speed in the hour of the day corresponding to the tth time step to the mean daily wind speed. Hourly wind speeds, $v_i(t)$, are generated from the mean daily wind speed realizations and $\alpha_i(t)$, as well as a term that considers the deviation from $\alpha_i(t-1)$ in the prior time step to preserve temporal correlations, and a random variable term:

$$\begin{aligned} v_i(t) = {} & \beta_i\left[v_i(t-1) - u_{i,k}(d(t-1))\alpha_i(t-1)\right] \\ & + u_{i,k}(d(t))\alpha_i(t) + \tilde{y}_i \end{aligned} \tag{7}$$

where $\tilde{y}_i \sim \mathcal{N}(0, \sigma_{y,i}^2)$ and β_i and $\alpha_{y,i}$ are calculated by a least-squares fit of the model to the hourly wind dataset. The day-ahead forecast for each hour, $\widehat{v}_i(t)$, is produced using the same model, but using the forecasted mean daily wind speed and excluding the random variable term:

$$\widehat{v}_i(t) = \widehat{u}_i(d(t))\alpha_i(t) + \beta_i\left[\widehat{v}_i(t-1) - \widehat{u}_i(d(t-1))\alpha_i(t-1)\right] \tag{8}$$

Maintaining the appropriate geographical and temporal correlations in the irradiance model is complicated by the fact that both the direct normal irradiance (DNI) and the diffuse horizontal irradiance (DHI) are required for the calculation of power output from solar systems, while most studies of solar forecasting accuracy report the errors in the mean daily global horizontal irradiance (GHI). To account for these inconsistencies, the model assumes that the system operator is provided with a day-ahead forecast of the mean daily GHI and builds forecasts of hourly data from historical data and a simple model. Rather than approximating the DNI and the DHI from the GHI and a clear-sky model, a statistical approach is employed to account for the temporal and geographical variations in both the clear-sky irradiance and the effects of cloud cover. Mean daily GHI realizations are produced using a method similar to that used to calculate mean daily wind speeds, with the Cholesky decomposition of the correlation matrix formed from the historical irradiance data. A statistical model based on several years of irradiance data is then used to produce the hourly DNI on each day, and a location- and time-dependent affine function is used to generate

the DHI from the DNI on each hour at each site. The details of this statistical approach are described in the Supplemental Information.

The production of load realizations is simplified by the availability of historical day-ahead hourly load forecast data from the California ISO. The model assumes that the load at each time step, $L(t)$ can be approximated by a function of the forecasted load, $\widehat{L}(t)$, the forecast error in the prior time step, and a random variable term:

$$L(t) = \gamma_1 \widehat{L}(t) + \gamma_2 \left[L(t-1) - \widehat{L}(t-1) \right] + \tilde{z} \tag{9}$$

where $\tilde{z} \sim \mathcal{N}(0, \sigma_L^2)$, and γ_1, γ_2, and σ_L are calculated using a least-squares fit of the model to historical hourly load and load forecast data.

Forced outages of conventional generators are included in the simulation by sampling the binomial distribution. For a generator type b, the available power generation in the k^{th} realization, $P_{b,k}(t)$ is calculated as:

$$P_{b,k}(t) = \tilde{\nu}_b P_b^{\text{unit}} \tag{10}$$

where P_b^{unit} is the average generator unit size and $\tilde{\nu}_b$ is a binomially-distributed random variable:

$$\tilde{\nu}_b \sim \beta \left(ceil \left[\frac{P_b^{\text{tot}}}{P_b^{\text{unit}}} \right], 1 - q_b \right) \tag{11}$$

This distribution depends on the forced outage rate, q_b, and the total installed capacity, P_b^{tot}. This method assumes that forced outages are independent events.

2.6. Carbon emissions analysis

With the output of the model, a more detailed analysis of the carbon emissions reductions can be undertaken using the framework presented in [22]. Katzenstein and Apt describe a parameter, η, which represents the fraction of expected emissions reductions achievable from the displacement of carbon-based generation with wind and solar power. They found that η is approximately 76% for systems in which natural gas is used with wind and solar plants to provide baseload power. That is, for a 1% increase in the energy penetration of wind or solar, the carbon emissions are reduced by only 0.76% due to the emissions associated with spinning reserves. Applying a similar methodology to the portfolios presented in this study, it is possible to quantify the fraction of the expected emissions reductions than can be achieved in stochastic systems in which variable renewables are used with a diverse conventional generating portfolio to supply a time-dependent load. Because the generator portfolios are more diverse in this study, the baseline expected emissions reductions are determined by making the deterministic assumption, rather than scaling the emissions according to the penetration factor.

To sample different penetration levels, the capacities of wind and solar produced for the low-carbon portfolios are uniformly scaled by factors between 0 and 1 prior to running the dispatch simulation. The generation composition and emissions data provided by these simulations is used to build a plot of the carbon intensity (in tCO_2 per GWh) versus the penetration of wind and solar power. The error associated with the deterministic assumption is determined by comparing the slopes of the emissions versus penetration curves derived from the stochastic simulations and from the deterministic analyses. The deterministic simulations are run using the same renewable portfolios that are used to build the stochastic emissions curve. However, the dispatch simulation considers only one realization in which the meteorological and load conditions match the input hourly data and day-ahead forecasts have zero error.

3. Model inputs and data

In this study, the model was run for the California ISO operating area using hourly data from 2005 to 2006. All inputs and data were obtained from public sources. Historical hourly forecasted and actual load data was obtained from the California ISO via the OASIS database [28]. Projected 2050 load data was approximated by applying an affine function to the 2005 and 2006 load data to match a peak demand that grows at an annual rate of 1.12% and an annual generation that grows at a rate of 0.82% per year from 2010 to 2050 [29]. Modeled wind speed data were obtained from the Western Wind Dataset (WWD) [30]. This dataset includes hourly 100-m wind speed data produced using the Weather Research and Forecasting (WRF) model with a 2 km × 2 km resolution, regridded to 1 arc-second. The WWD provides data at sites chosen based on their developability, proximity to planned transmission projects, and wind power density [31]. The model presented here considers the 200 largest clusters of aggregated WWD sites in California and assumes the same capacity density assumed in the WWD (7.5 W-installed/m^2). This amounts to a maximum potential wind development of 73.6 GW over approximately 10,000 km^2 (2.5% of California's total land area).

Solar irradiance data for 2005 were obtained from the 1991–2005 National Solar Radiation Database (NSRDB), which was derived from meteorological data from the National Climatic Data Center and the Meteorological-Statistical (METSTAT) model [32]. Data were obtained for all NSRDB stations in California. Solar data for 2006 were obtained from the Solar Anywhere database [33], which provides data produced using the SUNY model with a 10 km × 10 km resolution [34,35]. Data were selected from grid boxes containing the California NSRDB stations.

Potential solar thermal sites were chosen based on the locations and sizes of proposed large-scale solar projects throughout California [36] and the Solar Energy Study Zones identified by the Bureau of Land Management as suitable sites for the development of solar [37]. The maximum installed capacity at each site was calculated assuming a ratio of 47.2 W-installed/m^2, which is consistent with data from the SEG VI system [38], yielding a total potential capacity of 76.2 GW over 1600 km^2 (0.4% of California's land area). For each solar thermal site, irradiance data are used from the nearest NSRDB station. For the photovoltaic study, the average hourly irradiance for each county was calculated from the hourly irradiance data at the NSRDB stations in each county in the California ISO operating area and weighted according to the county-wide development potential [39] in order to construct the state-wide aggregated solar PV hourly resource. This yielded a maximum capacity of residential and commercial photovoltaics of 28.2 GW.

Temperature data are also required in order to calculate the expected output of photovoltaic systems. Because hourly temperature data are not publicly available for the time period of interest, a simple linear model was built to approximate the hourly temperature as a function of the temperature in the prior hour, the average daily temperature, and the GHI. This model was built using hourly temperature and irradiance data from the NSRDB Typical Meteorological Year [40].

The hydroelectric generation model requires as input the approximate daily generation from both large-scale and small-scale hydroelectric plants. These data are not publicly available, but can be approximated from the daily discharge for power generation data provided by the California Department of Water Resources (DWR) through the California Data Exchange Center [41] and

Table 1
Cost data used for the 2005 scenarios. All costs are presented in 2006$.

Technology	Capital ($/kW)	Fixed O&M ($/kW-yr)	Variable O&M ($/MWh)	Fuel ($/MBtu)	Reference
Hydroelectric	1408	13.57	3.41	0	[21]
Geothermal	3300	253.9	0	0	[21]
Natural Gas	792	14.62	3.05	6.53	[21,46]
Wind	1675	11.68	7.11	0	[21]
Photovoltaic	5335	74.69	0	0	[21]
Solar Thermal					
Solar Field	1839	0	0	0	[47]
Power Plant	2321	0	27.37	0	[47]
Storage	22.42[a]	53.35[a]	0	0	[24]

[a] Storage capital cost is in $/kWh and fixed O&M cost is in $/kWh-yr.

nameplate capacity data from the Bureau of Reclamation [42]. The total state-wide installed capacities of conventional and pumped-storage hydroelectric plants were obtained from the Energy Information Agency [43] and the proportion of the conventional capacity that qualifies as small hydroelectric power was approximated by solving for the capacities that best reproduce the capacity factor obtained from [43], given the generation profiles approximated from the DWR discharge data. An additional 7,000 MW of large-scale hydroelectric power was added to approximate the imported generation from the Pacific Northwest [44]. These assumptions resulted in a total capacity of in-state and imported hydroelectric power of 20.8 GW.

Geothermal resource data for California were obtained from a California Energy Commission study that includes resource estimates for dry steam, dual flash, and binary plants totaling to a maximum capacity of 4825 MW [45]. Cost data for the 2005 scenarios were obtained from the literature and are listed (with references) in Table 1. Cost projections for the 2050 scenarios were produced by scaling the 2005 cost data by the same ratios used in the ReEDS study to project from 2005 to 2050 [21]. The 2050 scenario also includes a 100$/t$CO_2$ cost of carbon. Most notable in the 2050 cost projection is a 70% decrease in the capital cost of distributed photovoltaics.

4. Results and discussion

The model was run in both least-cost and least-carbon modes for two load and cost function scenarios to produce low-cost and low-carbon portfolios for each scenario. The 2005 scenario was simulated using the cost functions in Table 1 and the historical load data from the California ISO. A 2050 scenario was also simulated using the 2050 projected cost functions and projected load data described in Section 3. These portfolios are not intended to represent forecasts, but are instead used to elucidate planning and operational issues that arise for systems with different load characteristics and penetrations of variable renewables. System-level results from the four simulations are shown in Table 2. The energy and capacity compositions of the four portfolios are shown in Fig. 3 (a) and (b), respectively. The low-carbon portfolio for 2005 is marked by substantial increases in the installed capacities of wind (73.6 GW) and solar (48 GW) power. Most of the generation from natural gas in the low-cost portfolio is displaced by wind power in the low-carbon portfolio, as solar power yields low capacity factors due to curtailment in hours when wind power alone provides sufficient generation to meet the load. The 2050 low-cost portfolio boasts significant installed capacities of wind (35.1 GW) and solar (36.7 GW) due to the projected reduction in costs of the these technologies and the high cost of carbon, while the 2050 low-carbon portfolio requires the development of all potential wind and solar capacity.

The 2005 low-carbon portfolio is capable of meeting the 2005 California ISO demand with 99.8 ± 0.2% of the energy generated by non-carbon-based technologies, while the 2050 low-carbon scenario provides 95.9 ± 0.4% of the delivered energy from non-carbon-based technologies. The hourly generation mix on four randomly selected days in this low-carbon 2050 simulation are shown in Fig. 4. Both low-carbon portfolios are characterized by very large system-wide generating capacities; the 2005 low-carbon scenario requires over 2.5 times California's actual generating capacity in 2005. The significant increase in capacity that accompanies high penetration grid integration of variable renewables will necessarily require substantial investments in updating and expanding transmission and distribution infrastructure.

More specific results from the 2050 low-carbon portfolio, including capacity, fraction of total annual generation, and capacity factor for each type of generating technology are shown in Table 3. The dramatic increase in installed capacity required to mitigate the variability and uncertainty in generation in this low-carbon system is a consequence of the relatively low capacity factors of wind and solar and the large reserve requirements associated with their grid integration. The capacity factors of wind and solar are further reduced by allowing curtailment in hours when resource availability exceeds demand. The 2.6% capacity factor for natural gas plants also indicates that mitigating intermittency with conventional technology may require a new operating paradigm for dispatchable plants, in which reliable capacity is valued over energy generation. The successful grid integration of very large-scale intermittent renewables with conventional generating technology will therefore likely require expanded capacity-based markets.

The model also determines that the installed capacity of natural gas decreases only slightly between the low-cost and low-carbon solutions, while the share of generation from natural gas decreases

Table 2
System-level model results from low-carbon and low-cost portfolios produced for 2005 and 2050 scenarios, juxtaposed with the statistics from the actual California electric power sector in 2005. Results for the 2005 and 2050 scenarios are averaged over the two-year simulation period and account only for the California ISO operating area. CO_2-free technologies include wind, solar thermal, photovoltaic, all hydroelectric, and geothermal. This category also includes nuclear and biomass for the actual 2005 portfolio. "Renewable" technologies include wind, solar thermal, photovoltaic, small hydroelectric, and geothermal. This category also includes biomass for the actual 2005 portfolio. Uncertainties are derived from the standard deviations of the model output across all Monte Carlo realizations, where it exceeds the precision of the reported data.

	2005 Scenarios		2050 Scenarios		Actual 2005
	Low-CO_2	Low-cost	Low-CO_2	Low-Cost	System [43]
Delivered Energy Composition					
CO_2-free Generation (%)	99.8 ± 0.2	39.9 ± 0.1	95.9 ± 0.4	64.6 ± 0.4	49.7
"Renewable" Generation (%)	78.6 ± 0.2	18.8 ± 0.1	82.8 ± 0.4	51.4 ± 0.4	11.8
Carbon Emissions					
Annual Emissions ($\times 10^6$ tCO_2)	10.2 ± 0.1	58.2 ± 0.1	35.9 ± 0.1	68.9 ± 0.1	54.7
CO_2 Intensity (tCO_2/GWh)	43.2 ± 0.1	247 ± 1	94.2 ± 0.1	181 ± 1	273
Generator Statistics					
Total Capacity (GW)	174.3 ± 0.1	68.4 ± 0.1	281.7 ± 0.1	182.0 ± 0.1	66.1
Average Capacity Factor (%)	16.6 ± 0.1	42.4 ± 0.1	16.5 ± 0.1	25.6 ± 0.1	34.6

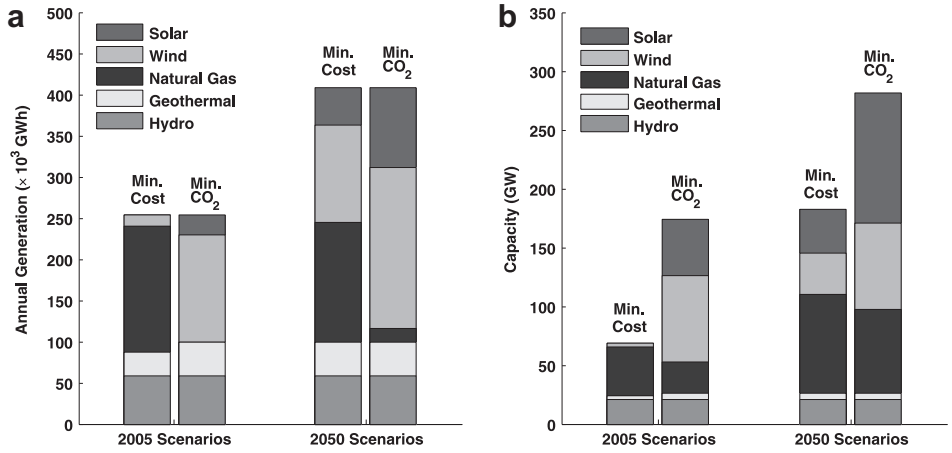

Fig. 3. (a) Energy and (b) Capacity composition of each portfolio calculated using the full stochastic model. Solar power includes centralized solar thermal plants as well as commercial and residential rooftop photovoltaics. Natural gas power includes both Class I and Class II plants. Hydropower includes in-state and imported large-scale, small-scale, and pumped-storage hydro.

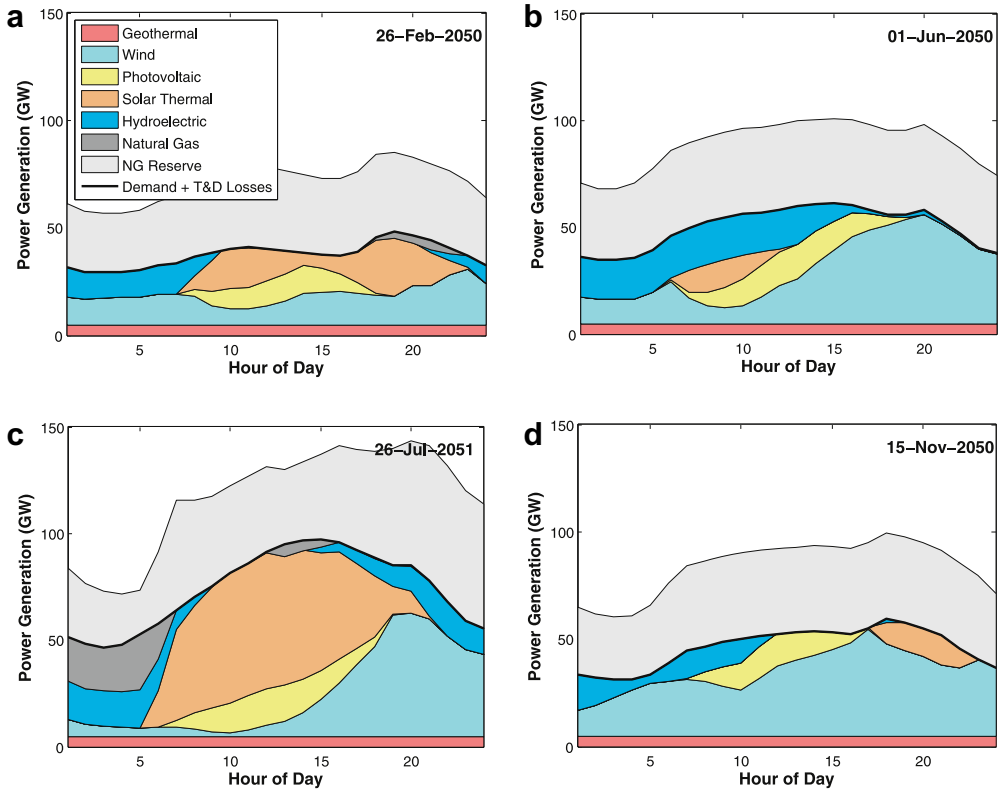

Fig. 4. Real-time power dispatch by generation technology on four days throughout the 2050 simulation period based on the low-carbon portfolio. The days were selected randomly from each season.

Table 3
Generator fleet statistics by technology, calculated by the model for the 2050 low-carbon portfolio. Uncertainties are derived from the standard deviations of the model output across all Monte Carlo realizations unless this uncertainty is smaller than the precision of the reported data.

Generating Technology	Installed Capacity (GW)	Share of Generation (%)	Capacity Factor (%)
Solar	110.5	24 ± 1	10.1 ± 0.4
Wind	73.6	48 ± 1	30.3 ± 0.8
Natural Gas	72.0	4.0 ± 0.5	2.6 ± 0.4
Geothermal	4.8	10.2 ± 0.1	98.8 ± 0.1
Hydroelectric	20.8	14.1 ± 0.1	31.7 ± 0.1

dramatically (by over 99% in 2005 and 88% in 2050). Furthermore these results demonstrate that the large capacities of dispatchable generation that are required to balance the load in systems with very high penetrations of variable renewables do not preclude dramatic reductions in the carbon emissions associated with system operation. The 2005 low-carbon portfolio achieves an 81% reduction in electric power sector carbon emissions from 2005 levels and the 2050 low-carbon portfolio meets a 34% reduction in emissions from 2005 levels.

The results from applying the carbon emissions analysis described in Section 2.6 to the 2005 scenario are shown in Fig. 4.

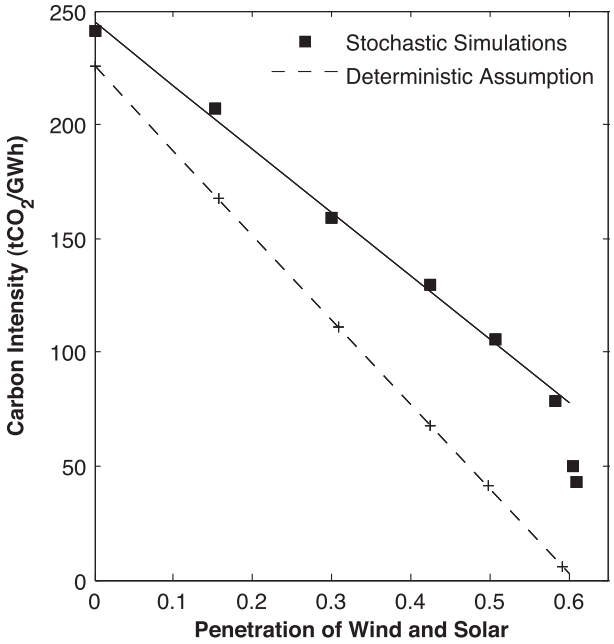

Fig. 5. System-wide carbon dioxide emissions (per GWh of generated energy), as a function of the energy penetration of wind and solar power in 2005–2006. The solid line is a least-squares linear fit to results from the stochastic simulations with penetrations less than 60%. The dashed line is a least-squares linear fit to the results from the deterministic simulations.

The stochastic simulations suggest that for energy penetrations of wind and solar less than 60%, the system-wide emissions can be reduced by 2.8 tCO_2/GWh for every 1% increase in the penetration level. The deterministic simulations yield a carbon emissions reduction rate of 3.7 tCO_2/GWh per 1% of wind and solar penetration, suggesting that deterministic grid integration studies may overestimate the achievable carbon emissions reductions by approximately 33%. Exceeding a 60% energy penetration of wind and solar in these simulations was inhibited by the inclusion of additional non-carbon-based technologies like hydropower and geothermal power, but as the installed capacities of wind and solar continue to increase, the emissions can be further reduced to 43.2 tCO_2/GWh due to a reduction in the natural gas reserve requirements (Fig. 5).

5. Conclusions

A new Monte Carlo-based grid integration model has been described that is capable of planning and providing analyses of systems with large penetrations of variable renewables combined with conventional generators that meet a time-dependent load with a specified reliability. This model has been applied to the California ISO operating area to identify a portfolio capable of providing 99.8% of the 2005–2006 generation with non-carbon-based technologies, including wind, solar thermal, photovoltaics, geothermal, and hydropower. This system is expected to achieve an 81% reduction in electric power sector carbon emissions from 2005 levels. A comparison of the model results with deterministic analyses shows that deterministic analyses may overestimate the achievable carbon emissions reductions by approximately 33%.

The low-carbon systems described in this study require large capacities of dispatchable generation with very low capacity factors. As a consequence of the low capacity factor fleets required by these systems, expanded capacity-based markets are expected to aid in achieving high penetrations of variable renewables. The large system-wide capacities of these systems will also require significant investments in transmission and distribution infrastructure to reliably bring the generation to load centers.

Furthermore this work has shown that significant carbon emissions reductions can be achieved with variable renewables, even when natural gas provides the requisite dispatchable capacity. This work also suggests that if high penetration variable renewables are used to reduce electric power sector emissions, then further reductions in emissions will rely on new technologies that can replace the capacity-based role provided by natural gas in these simulations. That is, in the context of a highly variable generation portfolio, clean technologies with reliably large capacities, but low (to zero) annual generation may better contribute to emissions reductions than clean technologies that boast larger capacity factors. Further reductions in electric power sector carbon emissions might therefore be met with high penetration demand response, vehicle-to-grid systems, and/or energy storage systems, in addition to efficiency improvements.

Future work with this model will be directed towards characterizing additional renewable portfolios, performing sensitivity studies with these portfolios, and modeling emerging technologies. The carbon emissions curves used to compare the stochastic solutions to the deterministic results in this study can also be used to compare the relative carbon abatement potential of both conventional renewable technologies and emerging technologies. This will provide a quantitative approach to comparing different clean generating technologies and exploring potential synergies between technologies.

Acknowledgments

This work was supported by the Precourt Institute for Energy Efficiency, the National Science Foundation Graduate Research Fellowship, and the Stanford Graduate Fellowship. The authors would like to thank Eric Stoutenburg, Gilbert Masters, and Nicholas Jenkins for their insights throughout this project and for their help in the preparation of this manuscript.

Appendix. Supplementary material

Supplementary data related to this article can be found online at doi:10.1016/j.renene.2011.01.015.

References

[1] Energy Information Administration. Annual energy outlook 2009, table a18, http://www.eia.doe.gov/oiaf/aeo/pdf/appendixes.pdf; 2009.
[2] Holttinen H, Meibom P, Orths A, Hulle FV, Ensslin C, Hofmann L, et al. Design and operation of power systems with large amounts of wind power, first results of IEA collaboration. In: 2006. Global Wind Power Conference. Adelaide, Australia.
[3] Connolly D, Lund H, Mathiesen B, Leahy M. A review of computer tools for analysing the integration of renewable energy into various energy systems. Applied Energy 2010;87(4):1059–82.
[4] Milligan M, Graham M. An enumerative technique for modeling wind power variations in production costing. In: 1997. International conference on probabilistic methods applied to power systems. Vancouver, BC.
[5] Milligan M, Porter K. The capacity value of wind in the United States: methods and implementation. The Electricity Journal 2006;19(2):91–9.
[6] Environmental Defense Fund. Elfin: electric utility production simulation and integrated planning system. Oakland, CA: Environmental Defense Fund; 1997. Tech. Rep.
[7] Maddaloni JD, Rowe AM, van Kooten GC. Wind integration into various generation mixtures. Renewable Energy 2009;34(3):807–14.
[8] DeCarolis JF, Keith DW. The economics of large-scale wind power in a carbon constrained world. Energy Policy 2006;34(4):395–410.
[9] Hirst E. Integrating wind output with bulk power operations and wholesale electricity markets. Wind Energy 2002;5(1):19–36.
[10] California Wind Energy Collaborative. California RPS integration cost analysis-phase 1: one year analysis of existing resources. California Energy Commission; 2003. Final Report CEC-500-03-108C.

[11] Lund H. Large-scale integration of optimal combinations of PV, wind and wave power into the electricity supply. Renewable Energy 2006;31(4):503–15.
[12] Czisch G, Giebel G. Realisable scenarios for a future electricity supply based 100% on renewable energies. In: 2004. Proceeding of the Risø International Energy Conference. Risø, DK.
[13] Hoste G, Dvorak M, Jacobson MZ. Matching hourly and peak demand by combining different renewable energy sources; 2009. [VPUE Final Report].
[14] Jacobson MZ. Review of solutions to global warming, air pollution, and energy security. Energy and Environmental Science 2009;2:148–73.
[15] Ekren O, Ekren BY. Size optimization of a PV/wind hybrid energy conversion system with battery storage using simulated annealing. Applied Energy 2010;87(2):592–8.
[16] Zhou W, Lou C, Li Z, Lu L, Yang H. Current status of research on optimum sizing of stand-alone hybrid solar-wind power generation systems. Applied Energy 2010;87(2):380–9.
[17] Weber C, Meibom P, Barth R, Brand H. Wilmar: a stochastic programming tool to analyze the large-scale integration of wind energy. In: Kallrath J, Pardalos P, Rebennack S, Scheidt M, editors. Optimization in the energy industry. Berlin: Springer Heidelber; 2009.
[18] Meibom P, Barth R, Brand H, Weber C. Wind power integration studies using a multistage stochastic electricity system model. In: 2007. IEEE Power Engineering Society General Meeting. Tampa, FL.
[19] Milligan M, Miller A, Chapman F. Estimating the economic value of wind forecasting to utilities. In: 1995. p. 285–94. Windpower 95 American Wind Energy Association Conference.
[20] Hirst E, Hild J. The value of wind energy as a function of wind capacity. The Electricity Journal 2004;17(6):11–20.
[21] Short W, Blair N, Sullivan P. Reeds model documentation: base case data and model description. Boulder, CO: National Renewable Energy Laboratory; 2008. Tech. Rep.
[22] Katzenstein W, Apt J. Air emissions due to wind and solar power. Environmental Science & Technology 2009;43(2):253–8.
[23] REPower Systems. Mm92 product brochure, http://www.repower.de/fileadmin/download/produkte/PP_MM92_uk.pdf; 2009.
[24] Pacheco JE, Showalter SK, Kolb WJ. Development of a molten-salt thermocline thermal storage system for parabolic trough plants. Journal of Solar Energy Engineering 2002;124(2):153–9, http://link.aip.org/link/?SLE/124/153/1.
[25] Masters G. Renewable and efficient electric power systems. Hoboken, NJ: John Wiley and Sons; 2004.
[26] Grant M, Boyd S. Graph implementations for nonsmooth convex programs. In: Blondel V, Boyd S, Kimura H, editors. Recent advances in learning and control. Lecture notes in control and information sciences. Springer-Verlag Limited. p. 95–110, http://stanford.edu/boyd/graph_dcp.html; 2008.
[27] Grant M, Boyd S. Cvx: Matlab software for disciplined convex programming, version 1.21, http://cvxr.com/cvx; 2009.
[28] California Independent System Operator. System load query, oasis database, http://oasishis.caiso.com; 2009.
[29] Kavalec C, Gorin T. California energy demand 2010–2020. Staff draft forecast CEC-200-2009-012-SD. California Energy Commission; 2009.
[30] 3TIER. Wind integration datasets, www.nrel.gov/wind/integrationdatasets; 2010.
[31] 3TIER. Development of regional wind resource and wind plant output datasets; 2010. NREL Subcontract Report SR-550–47676.
[32] Wilcox S, Marion W. National solar radiation database, 1999–2005: user's manual. National Renewable Energy Laboratory, http://www.nrel.gov/docs/fy07osti/41364.pdf; 2007. Technical Report TP-581–41364.
[33] Clean Power Research, LLC. SolarAnywhere, www.solaranywhere.com; 2010.
[34] Perez R, Ineichen P, Moore K, Kmiecik M, Chain C, George R, et al. A new operational satellite-to-irradiance model. Solar Energy 2002;73(5):307–17.
[35] Perez R, Schlemmer J, Renne D, Cowlin S, George R, Bandyopadhyay B. Validation of the suny satellite model in a meteosat environment. In: 2009. Proceedings of the ASES Annual Conference. Buffalo, New York.
[36] California Energy Commission. Large solar energy projects, http://www.energy.ca.gov/siting/solar/index.html; 2009.
[37] Bureau of Land Management. Solar energy study areas, http://www.blm.gov/wo/st/en/prog/energy/solar_energy/Solar_Energy_Study_Areas.html; 2009.
[38] National Renewable Energy Laboratory. Nrel troughnet: U.S. parabolic trough power plant data, http://www.nrel.gov/csp/troughnet/power_plant_data.html#segs_vi; 2009.
[39] Frantzis L, Graham S, Paidipati J. California rooftop photovoltaic (PV) resource assessment and growth potential by county. Navigant Consulting, California Energy Commission, http://www.energy.ca.gov/2007publications/CEC-500-2007-048/CEC-500-2007-048.PDF; 2007. PIER Final Project Report CEC-500-2007-048.
[40] Wilcox S, Marion W. Users manual for tmy3 data sets. National Renewable Energy Laboratory, http://www.nrel.gov/docs/fy08osti/43156.pdf; 2008. Technical Report TP-581–43156.
[41] Department of Water Resources. Historical data selector. California Data Exchange Center, http://cdec.water.ca.gov/selectQuery.html; 2009.
[42] Bureau of Reclamation. Hydroelectric powerplants listed by capacity, http://www.usbr.gov/power/data/faclcap.html; 2010.
[43] Energy Information Administration. Electric power annual 2007-data tables, http://www.eia.doe.gov/cneaf/electricity/epa/epa_sprdshts.html; 2009.
[44] Alvarado A, Griffin K. Revised methodology to estimate the generation resource mix of California electricity imports. California Energy Commission; 2007. Staff Paper CEC-700-2007-007.
[45] Sison-Lebrilla E, Tiangco V. Geothermal strategic value analysis. California Energy Commission; 2005. Staff Paper CEC-500-2005-105-SD.
[46] Energy Information Administration. Natural gas prices, California data tables, http://tonto.eia.doe.gov/dnav/ng/ng_pri_sum_dcu_SCA_a.htm; 2009.
[47] Enermodal Engineering Ltd. Cost reduction study for solar thermal power plants. Enermodal Engineering Ltd., Markbek Resource Consultants Ltd.; 1999. Final Report.